

## Synthesis and Characterization of Nanoferrite

S. G. DAHOTRE and L. N. SINGH

Department of Physics,  
Dr. Babasaheb Ambedkar Technological University,  
Maharashtra, INDIA.

(Received on: June 6, 2013)

### ABSTRACT

The effect of Zn substitution on the magnetic properties of  $Mn_{1-x}Zn_xFe_2O_4$  ferrites (where  $x=0$  to 1) were investigated by magnetization measurement. The samples were prepared by simple chemical technique of Sol-gel method. The saturation magnetization increases with increasing Zn content attaining a maximum value at  $x=0.6$  and then decreases thereafter. The X-ray diffraction pattern of the sample showed single phase cubic spinel structure. The IR spectra of the ferrites testify for homogeneity of the  $MnZnFe_2O_4$  spinel structure.

**Keywords:** Spinel structure, Magnetization.

### INTRODUCTION

Ferrite is nothing but a ferrimagnetic material. In the spinel structure, there are two different types of interstitial sites present, namely tetrahedral (A) and Octahedral (B), which are occupied by different metal ions. The magnetic properties of the spinel ferrites arise from the ability of these compounds to distribute the metal ions among the available tetrahedral (A) and Octahedral (B) sites<sup>1</sup>. Zinc ferrite has the normal spinel structure and is a class of soft magnetic material where as  $MnZnFe_2O_4$  is mixed ferrites in which 0.8% Mn is in A site, whereas 0.2 % of Mn goes in B site<sup>2</sup>. Smit and winj reported that in mixed Zn

ferrites like  $MnZnFe_2O_4$ , the A-B interaction is reduced with increasing Zn content, Zn substituted spinel ferrites showed good magnetic properties which are characterized by a maximum in saturation magnetization in certain composition<sup>3</sup>. Mn-Zn ferrites are interesting as they are exploited widely in microwave devices, magnetic recording media, and medical applications due to their high permeability (1000-2000) and low loss<sup>4</sup>.

### EXPERIMENTAL

Nanosize  $Mn_{1-x}Zn_xFe_2O_4$  ( $x=0$  to 1) were synthesized by chemical route i.e. sol-gel technique. The process has advantage of

inexpensive precursors, simple equipment, low temperature and resulting homogenous nanosized particles<sup>5</sup>. Analytical grade precursor salts of  $\text{MnCl}_2 \cdot 4\text{H}_2\text{O}$ ,  $\text{FeCl}_3 \cdot 6\text{H}_2\text{O}$ ,  $\text{ZnCl}_2 \cdot 4\text{H}_2\text{O}$  were taken in stoichiometric amounts and dissolved in 75 ml of distilled water.  $\text{P}^{\text{H}}$  of solution was varied between 2-3 as it plays crucial role for producing sample in nanosize. At lower  $\text{P}^{\text{H}}$ , precipitation of Mn is incomplete and for higher  $\text{P}^{\text{H}}$ , there may be zinc loss therefore optimum  $\text{P}^{\text{H}}$  for gel formation of solution was found to lie between 2 to 3. The activation energy for formation of ferrites of different metals is not equal. Activation energy calculated from kinetics of the formation reactions for different ferrites in temperature range of 20-100°C decreases in following sequence.  $E_{\text{A}}(\text{MnF}) > E_{\text{A}}(\text{ZnF})$ . Thus it should be concluded that the heating at temperature closer to 100°C is preferable for an easier and more rapid formation of Mn-Zn ferrite. During heating we add citric acid which removes the insoluble residue with formation of cation citric acid complex and holds the metal ions together. Ethylene glycol has also been added for homogeneity. The gel was then dried in oven at 250°C for 12 hours and then calcined at 800°C. According to density and grain growth, it was found that the sintering temperature of nanosized Mn- Zn ferrite powder was about 800°C<sup>6</sup>. The phase identification was carried out using XRD with  $\text{Cu-K}\alpha$  radiation. Magnetic measurements for synthesized nanoferrite was taken on VSM.

## RESULTS AND DISCUSSION

X-ray diffraction is a powerful technique used to uniquely identify the crystalline phases present in materials. From

$2\theta$  values for reflection, 'd' values were calculated using Bragg's equation and average crystallite size calculated of ferrite nanoparticles by Scherer's equation

$$D = \frac{0.9\lambda}{\beta \cos \theta}$$

It has been observed from XRD as Zn substitution increases crystallite size decreases which is shown in fig.1. It has been reported that the particle size of ferrite is influenced by the oxidation rate of the  $\text{Fe}^{2+}$  ions and also strong chemical affinity of specific cations like  $\text{Zn}^{2+}$  occupancy in tetrahedral site<sup>7</sup>.

| Zn Conc.(x) | Crystallite Size(nm) |
|-------------|----------------------|
| 0           | 156                  |
| 0.2         | 50                   |
| 0.35        | 133                  |
| 0.4         | 82                   |
| 0.5         | 83                   |
| 0.6         | 41                   |
| 0.7         | 62                   |
| 1           | 62                   |

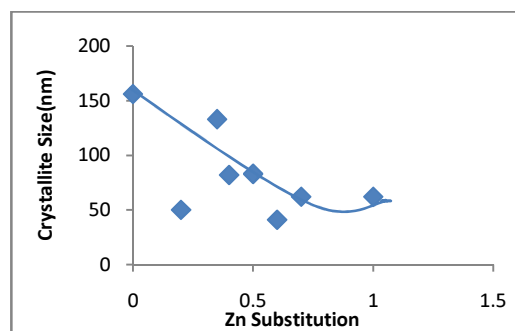


Fig.1: Graph of Zn substitution verses Crystallite size (nm)

The variation of lattice constant with Zn concentration is shown in fig. 2

| Zn Conc.(x) | Lattice parameter(A°) |
|-------------|-----------------------|
| 0           | 8.71                  |
| 0.2         | 7.62                  |
| 0.35        | 8.70                  |
| 0.5         | 7.19                  |
| 0.6         | 8.50                  |
| 0.7         | 8.08                  |
| 1           | 8.04                  |

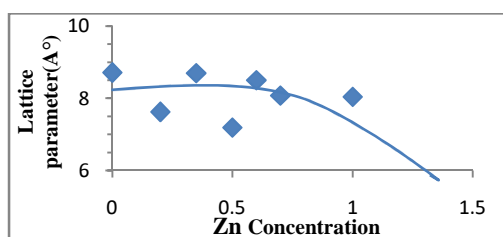


Fig.2: Graph of Zn Concentration versus Lattice parameter (A°)

It has been observed that lattice constant increases with decreasing Zn substitution due to replacement of  $\text{Zn}^{2+}$  cation having a smaller ionic radius (0.74nm) by  $\text{Mn}^{2+}$  cations having a larger one (0.082nm)<sup>8</sup>.

### Results of XRD calculations

| Zn<br>concent<br>ration<br>x | Cryst<br>allite<br>size<br>(nm) | Lattice<br>parameter (A°) |              | Crystal<br>Density<br>(gm /cc) |              |
|------------------------------|---------------------------------|---------------------------|--------------|--------------------------------|--------------|
|                              |                                 | Experi<br>mental          | Obser<br>ved | Experi<br>mental               | Obse<br>rved |
| 0                            | 156                             | 8.71                      | 8.50         | 4.64                           | 5.00         |
| 0.2                          | 35                              | 8.55                      | 8.51         | 4.96                           | 5.10         |
| 0.35                         | 133                             | 8.70                      | 8.49         | 4.72                           | 5.08         |
| 0.4                          | 82                              | 8.30                      | 8.40         | 5.40                           | 5.36         |
| 0.5                          | 83                              | 7.19                      | -            | 8.41                           | 5.30         |
| 0.6                          | 41                              | 8.07                      | 8.47         | 5.90                           | 5.16         |
| 0.7                          | 61                              | 8.08                      | 8.46         | 6.00                           | 5.24         |
| 1                            | 62                              | 8.04                      | 8.41         | 6.16                           | 5.38         |

The magnetic properties of the sample were studied at R. T. by using VSM.

The corresponding magnetization curves for different composition at RT are shown in fig.3

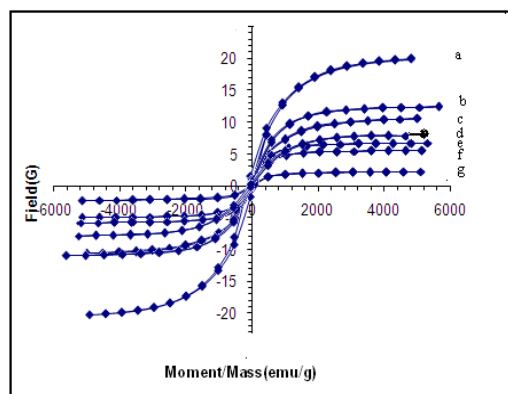


Fig 3: Room temperature magnetization curve of (a)  $\text{Mn}_{0.4}\text{Zn}_{0.6}\text{Fe}_2\text{O}_4$  (b)  $\text{Mn}_{0.5}\text{Zn}_{0.5}\text{Fe}_2\text{O}_4$  (c)  $\text{Mn}_{0.3}\text{Zn}_{0.7}\text{Fe}_2\text{O}_4$  (d)  $\text{ZnFe}_2\text{O}_4$  (e)  $\text{MnFe}_2\text{O}_4$  (f)  $\text{Mn}_{0.8}\text{Zn}_{0.2}\text{Fe}_2\text{O}_4$  (g)  $\text{Mn}_{0.6}\text{Zn}_{0.4}\text{Fe}_2\text{O}_4$

It has been observed that remenant magnetization and coercivity decreases with increasing Zn substitution and saturation magnetization initially increases and becomes maximum at  $x=0.6$  (21 emu/gm) and then decreases. When  $\text{Zn}^{2+}$  added, the experimental value of magnetic moment increases initially and then decreases which can be explained by Neel two sublattice theory for ferrimagnetism.

In addition the formation of dead layer on the surface, (due to environmental condition) non-saturation effects due to random distribution of particle size, presence of adsorbed water are also responsible for reducing the magnetization of Mn-Zn Nanoferrite shown in fig 3.<sup>9</sup> From, values of saturation magnetization, the magnetic moment per formula unit in Bohr magnetron was calculated using relation  $n_B = \frac{MM_s}{\mu_B N}$ . It

is observed that the saturation magnetization  $M_s$  and  $n_B$  increases with increases of Zn substitution upto  $x=0.6$  and decreases thereafter.

The value of saturation magnetization and magnetic moment is shown in table.

| Zn substitution | Saturation Magnetization (emu/gm) | $n_B$ |
|-----------------|-----------------------------------|-------|
| 0               | 7.04                              | 2.32  |
| 0.2             | 6.26                              | 2.08  |
| 0.5             | 12.62                             | 4.2   |
| 0.6             | 21.92                             | 7.4   |
| 0.7             | 10.59                             | 3.6   |
| 1               | 8.58                              | 2.96  |

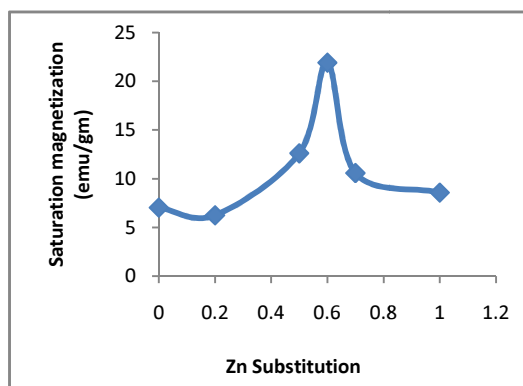


**Fig.4:** Variation of saturation magnetization with Zn substitution for  $Mn_{1-x}Zn_xFe_2O_4$  with  $x$  varying from 0 to 1

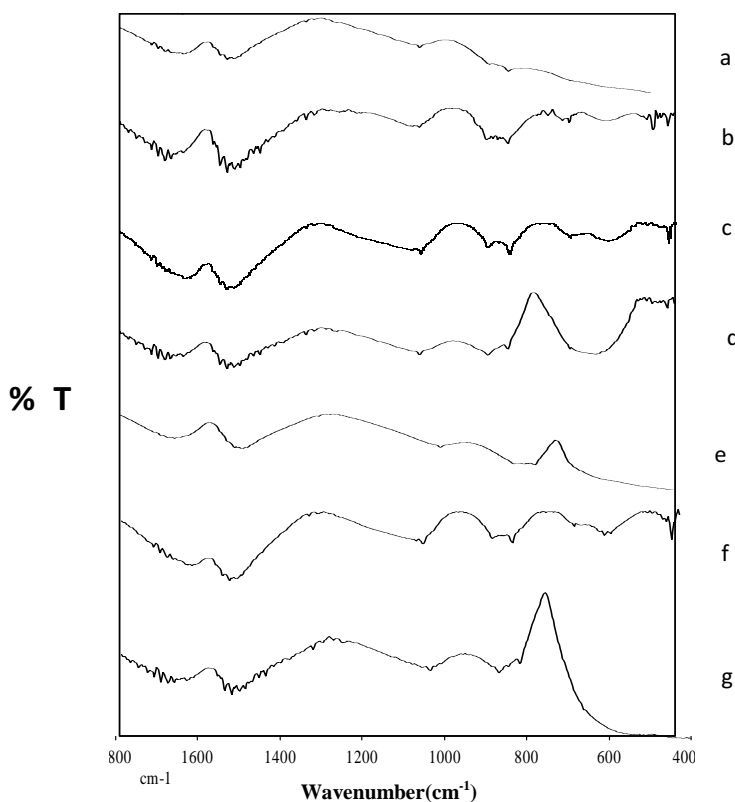


**Fig.5:** IR spectra of (a)  $ZnFe_2O_4$  (b)  $Mn_{0.4}Zn_{0.6}Fe_2O_4$  (c)  $Mn_{0.5}Zn_{0.5}Fe_2O_4$  (d)  $Mn_{0.6}Zn_{0.4}Fe_2O_4$  (e)  $Mn_{0.65}Zn_{0.35}Fe_2O_4$  (f)  $Mn_{0.8}Zn_{0.2}Fe_2O_4$  (g)  $MnFe_2O_4$

The characteristics bands of Mn-Zn ferrites are  $832\text{cm}^{-1}$  ( $\delta$  Zn-O-H) &  $946\text{cm}^{-1}$  ( $\delta$  Mn-O-H). The bands around  $1030\text{--}1122\text{cm}^{-1}$  attributed to ( $\delta$  Fe-O-H) are also shifted against the corresponding  $\gamma$ -  $\text{Fe}_2\text{O}_3$  bands thus reflecting the effect of  $\text{Zn}^{2+}$  and  $\text{Mn}^{2+}$  cations. Symmetric shape of the  $\gamma$ - Fe-O bands in the IR spectra of the ferrites testify for homogeneity of the  $\text{Mn}_{0.5}\text{Zn}_{0.5}\text{Fe}_2\text{O}_4$  spinel structure and uniformity of  $\text{Zn}^{2+}$  &  $\text{Mn}^{2+}$  distribution over the lattice<sup>10</sup>. IR absorption bands attributed to bending vibrations of OH groups directly connected to metal cations ( $\delta$  M-O-H) are known to be very sensitive to a degree of the structural perfection of composite oxides. Therefore, the region of IR spectra around the mentioned band can be used to evaluate the structural perfection of multi component spinel-type oxides. The IR absorption bands of solids in the range  $400 - 1000\text{cm}^{-1}$  are usually assigned to vibrations of ions in the crystal lattice. The vibrational spectra of spinel ferrites ( $\text{MFe}_2\text{O}_4$ ) are attributed to the high-frequency in the range  $400\text{--}2000\text{cm}^{-1}$  band ( $800\text{--}600\text{cm}^{-1}$ ) to the intrinsic vibration of the tetrahedral sites and the low frequency band ( $440\text{--}400\text{cm}^{-1}$ ) to the octahedral sites. The increase or decrease in the frequency of band is due to the fact that there is decrease or increase in the  $\text{Fe}^{3+}\text{-O}^{2-}$  bond length as a result of doping of  $\text{Zn}^{2+}$  ions.<sup>11</sup>

## CONCLUSION

X-ray diffraction measurements showed a good agreement between theoretical and experimental values of lattice constant and Crystal density for all composition. The average crystallite size was found to be 83 nm. The saturation

magnetization and magnetic moment is decreased after  $x=0.6$  indicates the possibility of a non-collinear spin canting effect in the system. Symmetric shape of the  $\gamma$  Fe-O bands in the IR spectra of the ferrites testify for homogeneity of the  $\text{Mn}_{0.5}\text{Zn}_{0.5}\text{Fe}_2\text{O}_4$  spinel structure and uniformity of  $\text{Zn}^{2+}$  and  $\text{Mn}^{2+}$  distribution over the lattice.

## REFERENCES

1. Mossbauer, X-ray and magnetization studies of  $\text{ZnAl}_x\text{Fe}_{2-x}\text{O}_4$  system. Suman Sharma & N. D. Sharma, *Indian J. of Pure and Applied Physics* Vol.44, PP-2 March (2006).
2. Intro. to magnetic materials, B. D. Cullity 20-226.
3. Effect of Zn on the magnetic ordering and Y-K angles of  $\text{Co}_{1-x}\text{Zn}_x\text{Fe}_2\text{O}_4$  ferrites, S.Noor Robul Islam, Sibendra Shakar Sikder, A.K.M. Abdul Hakim, S. Monjura Hoque, Saiduzzaman and Md. Obaidur Rahaman. *J of Mate. Sci. and Engg. A* 1,1000-10034 (2011).
4. Influence of oxidizer to fuel ratio on structural and magnetic properties. C. Murugeson, P.M.M. Dagzzali, G. Chandrashekharam. *J. of Mate.Sci. DOI* 10. 1007/s 10854- 013- 1222-2.
5. Z. X. Yue, W. Y. Guo, J.Zhou, Z. L. Gui L. T. Li, *J. of Magn & Magn. Mate.* 270, 216 (2004).
6. R. Arulmurugan, G. Vaidyana than, S. Dendhilnathan, B. Jeyadevan, *J. of Magn. & Magn. Material* 298, 83-94 (2006).
7. Dependence of Cation distribution, on a particle size, lattice parameter, and magnetic properties in nanosize Mn-Zn ferrites. C. Rath, S. Anand, R-P-Daas, K-K Sahu, S.D. Kulkarni, N.C. Mishra

- and S.K. Date. *J of applied Phy.* Vol-91, No. 4.
8. Effect of Zn on the Magnetic Ordering and Y-K Angles of  $\text{Co}_{1-x}\text{Zn}_x\text{Fe}_2\text{O}_4$  Ferrites. S. Noor, R. Islam, S.S. Sikder, A.K.M. Abdul Hakim, S. Monjura Hoque, Saiduzzaman & Md. Obaidur Rahaman *J. Mate. Sci. & Engg. A1*, 1000-1003 (2011).
  9. Mn-Zn Ferrite nanoparticles for ferro fluids preparation. R. Arulmuragan, G. Vaidyanathan, S. Sendhilnathan, B. Jegadevar, *J of M & MM* 298, 83-84 (2006).
  10. FTIR spectroscopic study of Biogenic Mn-Oxide formation by *Pseudomonas Putida* GB-1 S.J. Parikh and John Chrover, *Geomicrobiological J.*, 22, 207-218, (2005).
  11. Low Temperature Synthesis of nanosized  $\text{Mn}_{1-x}\text{Zn}_x\text{Fe}_2\text{O}_4$  ferrites & their characterization. R. Iyyer, R. Desai, R. V. Upadhyay. *Bull. Mate. Sci.* Vol 32, No.2, PP-141-147 April (2009).